Gene Expression Profiling of Liposarcoma Identifies Distinct Biological Types/Subtypes and Potential Therapeutic Targets in Well-Differentiated and Dedifferentiated Liposarcoma

Samuel Singer,[1] Nicholas D. Socci,[4] Grazia Ambrosini,[3] Elliot Sambol,[1] Penelope Decarolis,[1] Yuhsin Wu,[1] Rachael O'Connor,[1] Robert Maki,[3] Agnes Viale,[5] Chris Sander,[4] Gary K. Schwartz,[3] and Cristina R. Antonescu[2]

[1]Sarcoma Biology Laboratory, Sarcoma Disease Management Program, Department of Surgery, [2]Sarcoma Disease Management Program, Department of Pathology, [3]Laboratory of New Drug Development, Department of Medicine, and [4]Computational Biology Center, Memorial Sloan-Kettering Cancer Center and [5]Genomics Core Facility, Sloan-Kettering Institute, New York, New York

Abstract

Classification of liposarcoma into three biological types encompassing five subtypes, (*a*) well-differentiated/dedifferentiated, (*b*) myxoid/round cell, and (*c*) pleomorphic, based on morphologic features and cytogenetic aberrations, is widely accepted. However, diagnostic discordance remains even among expert sarcoma pathologists. We sought to develop a more systematic approach to liposarcoma classification based on gene expression analysis and to identify subtype-specific differentially expressed genes that may be involved in liposarcoma genesis/progression and serve as potential therapeutic targets. A classifier based on gene expression profiling was able to distinguish between liposarcoma subtypes, lipoma, and normal fat samples. A 142-gene predictor of tissue class was derived to automatically determine the class of an independent validation set of lipomatous samples and shows the feasibility of liposarcoma classification based entirely on gene expression monitoring. Differentially expressed genes for each liposarcoma subtype compared with normal fat were used to identify histology-specific candidate genes with an in-depth analysis of signaling pathways important to liposarcoma pathogenesis and progression in the well-differentiated/dedifferentiated subset. The activation of cell cycle and checkpoint pathways in well-differentiated/dedifferentiated liposarcoma provides several possible novel therapeutic strategies with MDM2 serving as a particularly promising target. We show that Nutlin-3a, an antagonist of MDM2, preferentially induces apoptosis and growth arrest in dedifferentiated liposarcoma cells compared with normal adipocytes. These results support the development of a clinical trial with MDM2 antagonists for liposarcoma subtypes which overexpress MDM2 and show the promise of using this expression dataset for new drug discovery in liposarcoma. [Cancer Res 2007;67(14):6626–36]

Introduction

Liposarcoma is the single most common soft tissue sarcoma and accounts for at least 20% of all sarcomas in adults (1). Liposarcomas are a heterogeneous group of mesenchymal tumors that may arise in any anatomic site. Surgery serves as the mainstay of therapy for localized liposarcoma. However, for locally advanced and disseminated disease there are few effective treatment options. Insight into the genetic events that drive the biology of these tumors may allow for molecular subtyping and the development of novel selective therapeutic strategies for advanced disease. Subtype is the most important determinant of clinical outcome (2–6); however, little is known about the genetic events specific to liposarcoma subtype. Widely used histopathologic and clinical criteria, such as liposarcoma subtype, location, age, and size, can be incorporated into liposarcoma-specific nomograms and used to estimate patient outcome (7). However, even in using such tools, a significant variability in predictive value exists among different clinical laboratories and hospitals with regard to the assessment of liposarcoma histologic subtype, which has been primarily based on morphologic appearance of the tumor.

Liposarcomas with similar morphologic appearance can follow different clinical courses and show divergent responses to systemic therapy. A correct histologic categorization is important because patients with pleomorphic liposarcoma have a 3-fold higher risk of distant metastasis compared with patients with dedifferentiated liposarcoma and are more likely to respond to treatment with systemic ifosfamide-based chemotherapy (8). However, the accurate discrimination of pleomorphic from dedifferentiated liposarcoma based on morphology alone is often a challenge even for an experienced soft tissue pathologist. Transcriptional profiling is a powerful tool for analyzing the relationships between tumors, discovering new tumor subgroups, assigning tumors to predefined classes, and predicting disease outcome. For this reason, we decided to develop a more systematic approach to the classification of liposarcoma based on gene expression analysis using microarrays.

Previous sarcoma gene expression profiling studies have shown that liposarcomas tended to cluster with malignant fibrous histiocytoma and leiomyosarcoma. However, these studies contained too few samples of any given liposarcoma subtype to draw clear distinctions specific to subtype (9, 10). A liposarcoma specific RNA expression profiling study compared eight pleomorphic liposarcomas to eight dedifferentiated liposarcomas and found no correlation between expression data and histologic subtype (11). In contrast, Matrix-CGH analysis provided unequivocal separation of dedifferentiated and pleomorphic subtypes, concluding that genomic profiling might be more advantageous than RNA expression analysis for subtype classification. Another liposarcoma-specific microarray study of 28 liposarcomas (11 well differentiated, 3 dedifferentiated, 7 myxoid, 7 round cell) and eight lipomas found by hierarchical clustering analysis that the dedifferentiated tumors formed a cluster

Note: Supplementary data for this article are available at Cancer Research Online (http://cancerres.aacrjournals.org/).

Requests for reprints: Samuel Singer, Memorial Sloan-Kettering Cancer Center, 1275 York Avenue, H1220, New York, NY 10021. Phone: 212-639-2940; Fax: 646-422-2300; E-mail: singers@mskcc.org.

doi:10.1158/0008-5472.CAN-07-0584

with the myxoid/round cell subtype and that the well-differentiated liposarcomas clustered with lipoma (12). In this study, they were unable to distinguish well-differentiated liposarcoma from lipoma based on gene expression profiles, and the incorrect grouping of dedifferentiated samples with myxoid/round cell tumors was most likely due to the limited sample numbers analyzed in this study. One of the major limitations of these liposarcoma array studies was the very limited sample number per subtype, and the fact that the same data set was used for both signature discovery and validation.

Here, we applied a microarray-based gene expression profiling approach to identify molecular signatures that distinguish liposarcoma subtype and developed a support vector machine (SVM) classifier demonstrating high discrimination accuracy between subtypes of liposarcoma, using a training set of 80 samples, and then validated this classifier on an independent test set of 49 lipomatous tissue samples. Differentially expressed genes for each liposarcoma subtype compared with normal fat were used to identify histology-specific signaling pathways and candidate genes important to liposarcoma pathogenesis and progression. We found significant activation of cell cycle and checkpoint pathways in well-differentiated and dedifferentiated liposarcoma subtypes compared with normal fat and postulated that several of these differentially expressed genes may serve as potential therapeutic targets. We then validated a particularly promising target, MDM2, and showed that Nutlin-3a, an MDM2 antagonist, induced substantial apoptosis and inhibited proliferation in dedifferentiated liposarcoma cell lines but showed no effects in human adipocyte cell lines. These data supports the clinical development of MDM2 antagonists for treatment of patients with well-differentiated/dedifferentiated liposarcoma.

Materials and Methods

Patient population and sample acquisition. Sequential patients seen at Memorial Sloan-Kettering Cancer Center between February 2002 and September 2005 for treatment of liposarcoma were evaluated for this study. Informed consent was obtained, and the project was approved by the local institutional review board (IRB protocol 02-060). Liposarcomas consist three biological types encompassing the five subtypes (well differentiated, dedifferentiated, myxoid, round cell, and pleomorphic). Lipomas and normal fat tissue were obtained at the time of surgical resection. Before RNA extraction, two 5-μm H&E histologic sections were cut from the top and bottom of the cryomold to assess for subtype, percentage of necrosis, cellularity, and normal/stromal tissue contamination. Regions chosen for analysis contained tumor cellularity of >75%, no mixed histology, and no area of necrosis or fibrosis.

RNA isolation and preparation for microarray analysis. A cryomold (0.5 cm × 1 cm × 1 cm), once typed for histology and macrodissected to assure subtype uniformity and to eliminate necrotic/normal tissue contamination, was used for RNA extraction and subsequent array analysis. Cryomold tumor samples were weighed and 1 mL of QIAzol lysis reagent was used for every 100 mg of tissue. The cryomold tissue specimens were then homogenized in QIAzol lysis reagent using Mixer Mill MM 300 (Retsch, Inc.) following standard procedures. After alcohol washing, the RNA sample was purified and eluted using the RNeasy Mini Spin Column from the RNeasy Lipid Tissue Mini kit (QIAGEN, Inc.). cDNA was synthesized in the presence of oligo(dT)24-T7 from Genset Corp. cRNA was prepared using biotinylated UTP and CTP and hybridized to HG U113A oligonucleotide arrays (Affymetrix, Inc.). Fluorescence was measured by laser confocal scanner (Agilent) and converted to signal intensity by means of Affymetrix Microarray Suite v5 software. The gene expression data are available at www.cbio.mskcc.org/Public/Liposarcoma.

Statistical methods and analysis. An unsupervised hierarchical clustering with $1 - \rho$ Pearson correlation distance function and ward linkage was used to investigate whether there was evidence for natural groupings of samples based on correlations between gene expression profiles. To assess the robustness, a parametric bootstrap resampling technique was used in which 1,000 bootstrap replicas for the original dataset were generated and clustered. A consensus tree was built from these 1000 bootstrap trees; the number at each node in the consensus tree indicates how many of the bootstrap trees had that subcluster. We then used the SVM supervised learning algorithm to classify the liposarcoma and normal fat samples. The SVM method computes the hyperplane that best discriminates between two groups by maximizing the distance to the closest points (margins). To make distinctions between these six tissue types, the classification problem is divided into a series of all 15 possible pair-wise comparisons. Each test sample is presented sequentially to these 15 pair-wise classifiers, which classify the sample into one of the pairs. A voting procedure is then used to determine into which group the sample belongs. We then evaluated the accuracy of this multiclass SVM-based classifier for liposarcoma subtype and normal fat diagnosis using a set of 69 liposarcomas and nine normal fat samples. To determine the optimal settings over the various variables, such as the number of genes (features) to use and the penalty cost function value, we use the cross-validation method. The idea is to divide the data into a training set and a test set. In our case, we used 10-fold cross validation, so the data was divided into a training set of 90% of the samples and at test set of 10%. This division is done randomly each time. We can then measure the performance for a given set of variable values by training on the training set and scoring on the test set. For the specific case of choosing the optimal number of genes to use, we ranked all the genes by their absolute t score and then tested models with varying numbers of genes from 1 to N (where N was roughly 100). Performance in the cross validation seemed to level off at about 15 genes per pair-wise classifier. The optimal SVM-based classifier was then tested on an independent blind test set of 49 lipomatous tissue specimens, consisting of 14 well differentiated, 13 dedifferentiated, 5 myxoid, 3 round cell, 6 pleomorphic liposarcoma, and 8 normal fat tissue samples.

Identification of therapeutic targets. The gene expression profiles from 10 patients with pure well-differentiated liposarcoma (no known dedifferentiated component), 10 patients with dedifferentiated liposarcoma, 10 patients with pure myxoid liposarcoma (no known round cell component), 10 patients with round cell liposarcoma, and 10 patients with pleomorphic liposarcoma were separately compared with the gene profiles from 10 patients with normal fat tissue. A gene discrimination analysis was done using a standard t test on the log of the expression signal. Genes were filtered by significance and on the fold change between the liposarcoma subtype and normal fat. To deal with the multiple testing problem, we used the false discovery rate (FDR) method to obtain corrected P values. Because the different comparison pairs gave vastly different significant levels, we picked cutoff values in the FDR for each comparison. In all cases, the cutoff was either 0.05 or smaller for the more significant comparisons. From each subtype-specific gene list, we selected potential therapeutic molecular targets that showed at least a 2-fold differential expression compared with normal fat. The Ingenuity Pathway Analysis application,[6] a web-based bioinformatic tool that maps gene lists (ranked by FDR or fold change) to a database of fully annotated biological interactions between genes displayed in a graphical format, was used to determine the significant gene interaction networks based on liposarcoma expression profiles. The most promising target genes in this pathway analysis were validated with quantitative reverse transcription–PCR (RT-PCR).

Expression quantification using real-time RT-PCR. This was done using the remaining RNA available after U133A chip hybridization. Extracted RNA was transcribed into cDNA using TaqMan RT reagents. One-step RT-PCR performs RT and PCR in a single-buffer system. Real-time analysis was used to quantitate gene expression. To compensate for potential degradation of target RNA and differences in the amount of starting material, real-time analysis was done in parallel on cDNA from each

[6] https://analysis.ingenuity.com

sample using rRNA as an endogenous control. The copy numbers obtained for the gene under study were divided by the corresponding copy numbers for the rRNA control to yield a normalized expression index. Real-time PCR was carried out according to the manufacturers' instructions, using an Applied Biosystems Prism 7900HT Sequence Detection System (Applied Biosystems). All primers/probes were designed using ABI Prism Primer Express 1.5 software (Applied Biosystems) with the probes spanning exonic junctions.

Cell culture and drug treatments. LS141 and DDLS cell lines were established from human dedifferentiated liposarcoma tissue samples. The normal human adipocyte (NADIP) cell line was established in culture from human s.c. fat tissue. Cells were grown in RPMI 1640, supplemented with 10% fetal bovine serum, 100 units/mL penicillin, and 100 μg/mL streptomycin and maintained at 37°C in 5% CO_2. The selective small-molecule antagonist of MDM2 nutlin-3a (13) was prepared as a 10 mmol/L stock solution in DMSO and stored at −20°C.

Proliferation assays. To evaluate the antiproliferative effect of nutlin exposure on LS141, DDLS, and NADIP cells, DNA content was estimated using the CyQuant Cell Proliferation kit (Molecular Probes). In brief, cells were plated in 96-well plates at a density of 2×10^4 cells per well and allowed to adhere overnight at 37°C. After treatment, cells were incubated with CyQuant dye and lysed. This dye exhibits strong fluorescence when bound to cellular nucleic acids, and, as such, the fluorescent signal is proportional to DNA content. Plates were read using the Spectramax M2 fluorescence microplate reader (Molecular Devices) at 480/520 nm excitation/emission.

Apoptosis assays. Evaluation of apoptosis was carried out using the Guava NexinTM kit (Guava Technologies) following the manufacturer's instructions. Briefly, cells were treated in duplicate 60-mm culture plates. Both adherent and floating cells were collected and washed once in cold PBS and once in 1× Annexin V binding buffer. Cells were then resuspended at a concentration of 1×10^6 cells/mL. Annexin V (5 μL) and 7-AAD (2.5 μL) were added to 50 μL of the cell suspension and allowed to incubate on ice for 30 min in the dark. The Annexin V–positive population was counted using the Guava perchloric acid (Guava Technologies), and data were analyzed using FloJo software (Tree Star, Inc.).

Immunoblotting. Cells were lysed in radioimmunoprecipitation assay buffer supplemented with protease inhibitor cocktail tablets (Complete Mini, Roche Diagnostics) and 1 mmol/L $NaVO_3$. Total protein concentration of the lysates was measured by Bio-Rad protein assay (Bio-Rad Laboratories), and equal amounts of protein were loaded on 4% to 12% PAGE gels (Invitrogen). Membranes were blotted with antibodies specific for MDM2, p53, and p21 (Santa Cruz Biotechnology, Inc.). The equal loading of protein was confirmed by Amido Black staining (Sigma Chemical) and Western blotting for α-tubulin (Upstate Biotechnology).

Results

Microarrays of liposarcoma group in distinct genomic clusters according to type and subtype. Here, we used microarrays to explore systematically the molecular variation underlying the biological and clinical heterogeneity in liposarcoma. Using Affymetrix U133A GeneChip arrays, we generated gene expression profiles for 69 liposarcomas, 7 lipomas, and 9 normal fat tissue specimens. Unsupervised hierarchical clustering was used to allow the dominant structure to dictate the separation of samples into clusters based on overall similarity in gene expression without prior knowledge of the sample identity (Fig. 1). This unsupervised clustering approach shows that the normal fat, lipoma, and liposarcoma subtypes form relatively discrete clusters. Three distinct global clusters were observed: (*a*) normal fat, lipoma, and well-differentiated liposarcoma; (*b*) dedifferentiated and pleomorphic liposarcoma; and (*c*) myxoid/round cell liposarcoma. Within the first cluster, lipomas form a distinct group from normal fat and well-differentiated liposarcoma. In this first global cluster, two well-differentiated liposarcoma clustered with the normal fat samples. For the second global cluster, most of the pleomorphic liposarcomas form a distinct subcluster from the dedifferentiated subtype. However, four dedifferentiated samples cluster with the pleomorphic samples and three well-differentiated samples cluster with dedifferentiated liposarcoma samples. In the third global cluster, two distinct subclusters are formed, one containing five myxoid and four round cell samples and the other subcluster containing 14 myxoid and five round cell liposarcoma samples.

Generation and validation of a SVM-based method for classification of liposarcoma and normal fat samples. We then used the supervised learning SVM algorithm to build a classifier to determine the subtype of liposarcoma cases and to show the feasibility of liposarcoma classification based entirely on gene expression measurements. A 10-fold cross-validation method was used to both test the performance and to determine the optimal number of genes to use. With 15 genes per pair-wise classifier (for a total of 142 genes), we were able to determine subtype with an accuracy of 90.8 ± 0.2% (see Supplementary Table S1 for 142 gene classifier). We then used this set of genes and validated the results on an independent test set of 49 lipomatous tissue specimens, consisting of 14 well differentiated, 13 dedifferentiated, 5 myxoid, 3 round cell, 6 pleomorphic liposarcoma, and 8 normal fat tissue

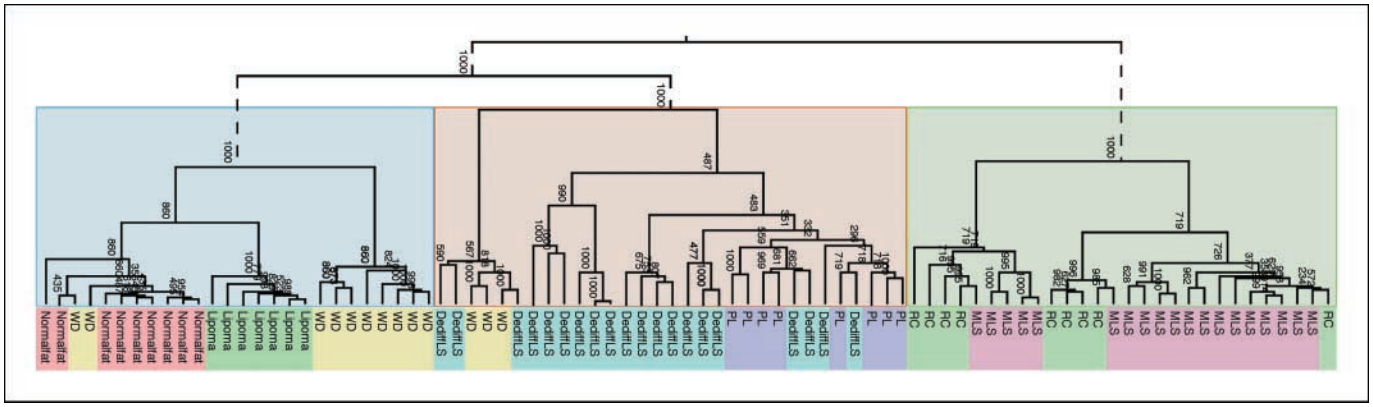

Figure 1. Hierarchical clustering of the liposarcoma, lipoma, and normal fat tissue expression data set. Before clustering, the data was filtered to remove genes that were scored absent in >75% of the samples, leaving 13,341 of the original 22,215 probe sets. Standard hierarchical clustering was done using the Pearson correlation to define the distance and ward linkage for the clustering. To assess the robustness, a parametric bootstrap resampling technique was used. The number at each node indicates how many of the bootstrap trees had that subcluster. Liposarcoma subtypes include well-differentiated (*WD*), dedifferentiated (*DediffLS*), myxoid (*MLS*), round cell (*RC*), and pleomorphic (*PL*).

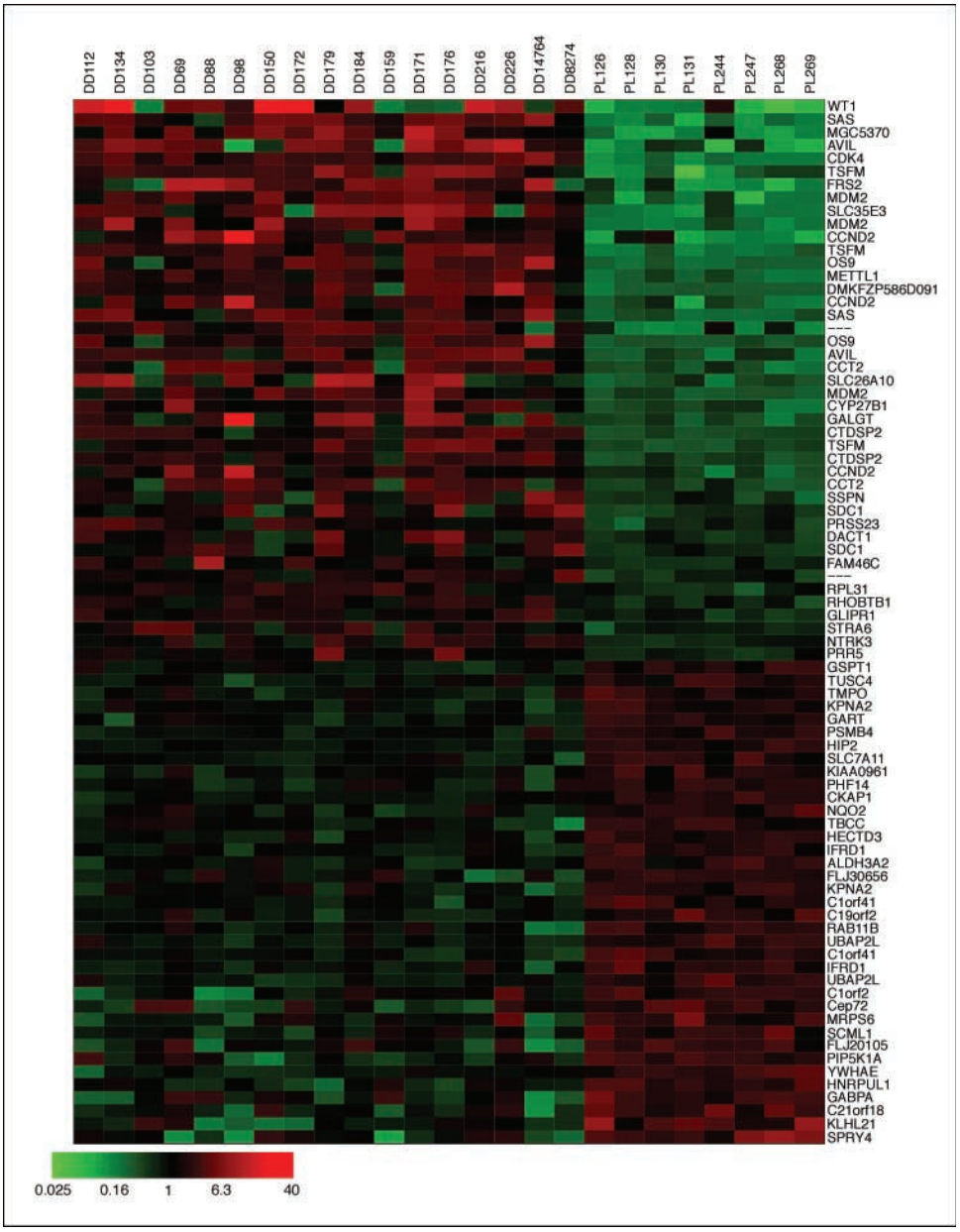

Figure 2. Eighty genes most highly differentially expressed comparing dedifferentiated to pleomorphic liposarcoma.

samples. This SVM classifier predicted the correct overall biological type of lipomatous tissue (normal fat versus well differentiated/dedifferentiated versus myxoid/round cell versus pleomorphic) for 45 of 49 samples (92%) and correctly identified the correct tissue subtype in 43 of 49 samples (86%). The misclassified biological types included one pleomorphic liposarcoma sample from the thigh that was misclassified as dedifferentiated liposarcoma, one dedifferentiated liposarcoma from the pelvis with 20% necrosis that was misclassified as pleomorphic and two well-differentiated liposarcomas one from the thigh and the other from the ankle that were misclassified as normal fat. The misclassified subtypes included one myxoid liposarcoma with increased cellularity that was misclassified as round cell, one retroperitoneal dedifferentiated liposarcoma sample misclassified as a well-differentiated liposarcoma, and one retroperitoneal well-differentiated liposarcoma with extensive myxoid change misclassified as a dedifferentiated liposarcoma. Subtype sample misclassification may be due to insufficient sampling or enhanced sensitivity of the gene expression analysis for progression of liposarcoma to a more aggressive, higher-grade subtype.

The list of the 15 most informative genes in the pleomorphic versus dedifferentiated liposarcoma SVM class predictor (see Supplementary Table S1, DD versus PL) was highly instructive with 12 genes located on the amplified chromosome 12 subregion 12q13-q15 commonly found in the large ring or marker chromosomes associated with dedifferentiated liposarcoma. The overexpressed genes in this subregion serve as the major feature used to discriminate these subtypes. The 80 genes significantly differentially expressed greater than 2-fold when comparing dedifferentiated with pleomorphic liposarcoma as shown in Fig. 2. Many of these differentially expressed genes encode proteins critical for controlling the G_1-S transition (*CDK4, MDM2, cyclin D1, cyclin D2, CCT2, GSPT1, CKS2, CKS1B*), regulation of G_2-M phase of cell cycle (*KPNA2, TUSC4*), growth factor receptors (*FRS2, NTRK3*), regulation of transcription [*WT1* (Wilms' tumor suppressor), *HIP2, SCML1,*

Table 1. Overexpressed genes in well-differentiated and dedifferentiated liposarcoma compared with normal fat

Gene	Title	Fold change
(*A*) Well-differentiated liposarcoma versus normal fat gene list		
ZIC1	Zic family member 1	37.2
TOP2A	Topoisomerase (DNA) II α 170 kDa	32.4
RRM2	Ribonucleotide reductase M2 polypeptide	18.1
FOXD1	Forkhead box D1	15.5
GAS41	Glioma-amplified sequence 41	13.7
CDK4	Cyclin-dependent kinase 4	11.6
MDM2	MDM2, p53 binding protein	10.2
CDKN2A	Cyclin-dependent kinase inhibitor 2A (p16)	9.0
HCAP-G	Chromosome condensation protein G	8.2
IGF-II	Insulin-like growth factor II	7.0
SAS	Sarcoma-amplified sequence	6.8
ARHGAP4	Rho GTPase-activating protein 4	5.7
TYMS	Thymidylate synthetase	5.3
MADL1	MAD2 mitotic arrest deficient-like	3.4
OS4	Conserved gene amplified in osteosarcoma	3.3
RACGAP1	Rac GTPase activating protein 1	3.3
RBL1	Retinoblastoma-like 1 (p107)	2.4
RAD17	RAD17 homologue, mitotic checkpoint	2.4
FUBP1	Far upstream element (FUSE) binding protein 1	2.3
BRCA2	Breast cancer 2, early onset	2.3
MARKS	Myristoylated alanine-rich protein kinase C substrate	2.2
IRS4	Insulin receptor substrate 4	2.2
CDC2	Cell division cycle 2, G_1-S and G_2-M	2.2
UBE2B	Ubiquitin-conjugating enzyme E2B (RAD6 homologue)	1.9
RAD1	RAD1 homologue, DNA damage response	1.7
(*B*) Dedifferentiated liposarcoma versus normal fat gene list		
TOP2A	Topoisomerase (DNA) II α 170 kDa	103.2
RRM2	Ribonucleotide reductase M2 polypeptide	38.5
HEC	Highly expressed in cancer	35.7
ZIC1	Zic family member 1 (odd-paired homologue, Dros.)	35.5
TRO	Trophinin	28.3
CDC2	Cell division cycle 2, G_1-S and G_2-M	19.9
FOXD1	Forkhead box D1	17.9
HCAP-G	Chromosome condensation protein G	17.2
CDK4	Cyclin-dependent kinase 4	14.0
MELK	Maternal embryonic leucine zipper kinase	13.3
CDC20	CDC20 cell division cycle 20 homologue, spindle	9.9
MDM2	Mdm2, p53 binding protein	9.6
TYMS	Thymidylate synthetase	9.2
CDKN2A	Cyclin-dependent kinase inhibitor 2A (p16)	7.7
CKS2	CDC28 protein kinase regulatory subunit 2	7.5
BUB1B	BUB1 budding uninhibited by benzimidazoles 1 homologue β	7.0
MAD2L1	MAD2 mitotic arrest deficient-like 1	6.3
RACGAP1	Rac GTPase-activating protein 1	6.1
SAS	Sarcoma-amplified sequence	5.7
CDH11	Cadherin 11, type 2, OB-cadherin (osteoblast)	5.2
RRM2	Ribonucleotide reductase M2 polypeptide	5.2
SOX4	Sex-determining region Y–box 4	4.7
CCNB2	Cyclin B2	4.3
SMO	Smoothened homologue (*Drosophila*)	3.4
TCF3	Transcription factor 3	3.4
CCNE2	Cyclin E2	3.2
BAX	BCL2-associated X protein	3.2
SSX2IP	Synovial sarcoma, X breakpoint 2 interacting protein	3.1
CDKN3	Cyclin-dependent kinase inhibitor 3 (CDK2-assoc dual specificity phosphatase)	2.9
UBE2C	Ubiquitin-conjugating enzyme E2C	2.9
GLI2	GLI-Kruppel family member GLI2	2.8

(*Continued on the following page*)

Table 1. Overexpressed genes in well-differentiated and dedifferentiated liposarcoma compared with normal fat (Cont'd)

Gene	Title	Fold change
RBL1	Retinoblastoma-like 1 (p107)	2.8
CKS1B	CDC28 protein kinase regulatory subunit 1B	2.8
MARKS	Myristoylated alanine-rich protein kinase C substrate	2.8
CCNB1	Cyclin B1	2.8
CDC7	CDC7 cell division cycle 7, G_1-S transition of mitotic cell cycle	2.7
FUBP1	FUSE binding protein 1	2.7
CALR	Calreticulin	2.6
PLOD	Procollagen-lysine, 2-oxoglutarate 5-dioxygenase	2.5
CDC25B	Cell division cycle 25B	2.5
RFC4	Replication factor C (activator 1) 4, 37 kDa, DNA replication	2.4
CHEK1	CHK1 checkpoint homologue, DNA damage response	2.0

NOTE: *A,* selected overexpressed genes from 251 genes that were differentially expressed with a FDR of <0.005, comparing the mean log gene expression levels in eight pure well-differentiated liposarcoma samples (no dedifferentiated component in sample or elsewhere in patient's tumor) to the mean gene log expression levels from nine normal fat tissue samples. *B,* selected overexpressed genes from the 130 genes that were differentially expressed with a FDR of $<1 \times 10^{-7}$ and >2-fold change, comparing the mean log gene expression levels of 20 pure dedifferentiated liposarcoma samples to those from nine normal fat tissue samples.

GABPA, and *WHSC1*] or known oncogenes [*RAB11B* (*RAS* oncogene family)], GTPase signal transduction, *SSPN*-sarcospan (*Kras* oncogene–associated gene)]. Supplementary Fig. S1 shows the list of 80 genes most highly correlated with well-differentiated/dedifferentiated class distinction. Many of the genes most useful for this distinction relate to the control of lipid, fatty acid, and carbohydrate metabolism (*PLIN, APM1, GPD1, LPL, ADH1B, LBP, PNPLA2, LIPE, ACSL1, DGAT1, CLU, APM2, FABP4, HK2, APOL6*), control of apoptosis (*CIDEA, SOCS3 MAPT, DAPK2, BAG2, BAX, BIRC5*-survivin, *SULF1*), cytoskeleton structural genes (*CKAP4, MAPT, FARP1, CTNNB1, ENC1, MARKS, TMP4, plectin1*), *RAS* pathway genes (*RAB23, HRASLS3, RAB20*), transcription factors (*PPARGC1A, PBX3, TLE4, SATB2, RBM9, FOXF2, ID3, FOXM1, SOX11*) or cell cycle control genes (*p130, cyclin H, MAPK1, CDC2, BUB1B, cyclin B2, CKS2, CDC20, DUSP4*). The progression of well-differentiated to dedifferentiated liposarcoma seems to be governed by the differential expression of key cell cycle, transcription factor genes, cytoskeleton/microtubule assembly, and apoptotic control genes. Together, these data suggest that genes useful for liposarcoma class prediction may also provide insight into liposarcoma pathogenesis and progression from low-grade to high-grade liposarcoma.

Results showing significant up-regulated genes in each liposarcoma subtype compared with normal fat. The genes differentially expressed for each liposarcoma subtype compared with normal fat can be used to identify candidate genes in liposarcoma differentiation and tumorigenesis and to identify new therapeutic molecular targets. Table 1*A* and *B* and Supplementary Tables S2 to S4 shows the significant up-regulated genes for each liposarcoma subtype compared with normal fat by comparing the mean log expression levels in each liposarcoma subtype samples with the normal fat tissue samples. To limit this gene list and to avoid multiple testing problem, we applied a stringent FDR for each subtype comparison and only examined genes that were differentially expressed more than 2-fold compared with normal fat.

Bioinformatic pathway analysis of differentially expressed genes in the three biological types of liposarcoma compared with normal fat reveals type-specific pathway alterations and potential therapeutic targets. The ingenuity pathway analysis application,[6] a web-based bioinformatic tool that maps gene lists (ranked by FDR or fold change) to a database of fully annotated biological interactions between genes displayed in a graphical format, was used to determine the significant gene interaction networks based on liposarcoma expression profiles. Comparison of gene expression in well-differentiated/dedifferentiated liposarcoma, myxoid/round cell liposarcoma, and pleomorphic liposarcoma with normal fat results in 998, 449, and 201 genes, respectively, that were differentially expressed more than 2-fold. These 998 genes for the well-differentiated/dedifferentiated type were entered into the ingenuity pathway analysis, resulting in 364 "focus genes" based on sufficient annotation of biological interactions. This final gene list resulted in 15 high-scoring interaction networks. Given the space limitations, we will present data from one of the most informative interaction networks in the well-differentiated/dedifferentiated subtype. Although there were several additional informative networks for all the biological types of liposarcoma, these will be developed in future publications. One of the most informative networks in this analysis contained a maximum of 35 genes, scored highly relative to other networks, and drew attention to several cell cycle and checkpoint genes, the majority of which are significantly over expressed in well-differentiated/dedifferentiated liposarcoma compared with normal fat (see Fig. 3*A*). *CDK4, MDM2, CDC2, CDC7, cyclin B1* (*CCNB1*), *cyclinB2* (*CCNB2*), *cyclin E2* (*CCNE2*), and key regulators of the cell cycle were significantly overexpressed in well-differentiated and dedifferentiated liposarcoma compared with normal fat and account for the high cellular proliferation found in these liposarcoma subtypes. Figure 3*B* depicts the differentially expressed genes in cell cycle regulation pathways specific to phases of the cell cycle in well-differentiated and dedifferentiated liposarcoma.

MDM2 as therapeutic target in well-differentiated/dedifferentiated liposarcoma. For these studies, we treated the two dedifferentiated liposarcoma cell lines with amplified MDM2 (LS141 and DDLS) and a NADIP cell line, which does not have amplified MDM2 with nutlin (5 μmol/L) for 1 to 5 days and cell viability was measured (Fig. 4*A*). As indicated, both of the dedifferentiated liposarcoma cell lines were highly sensitive to

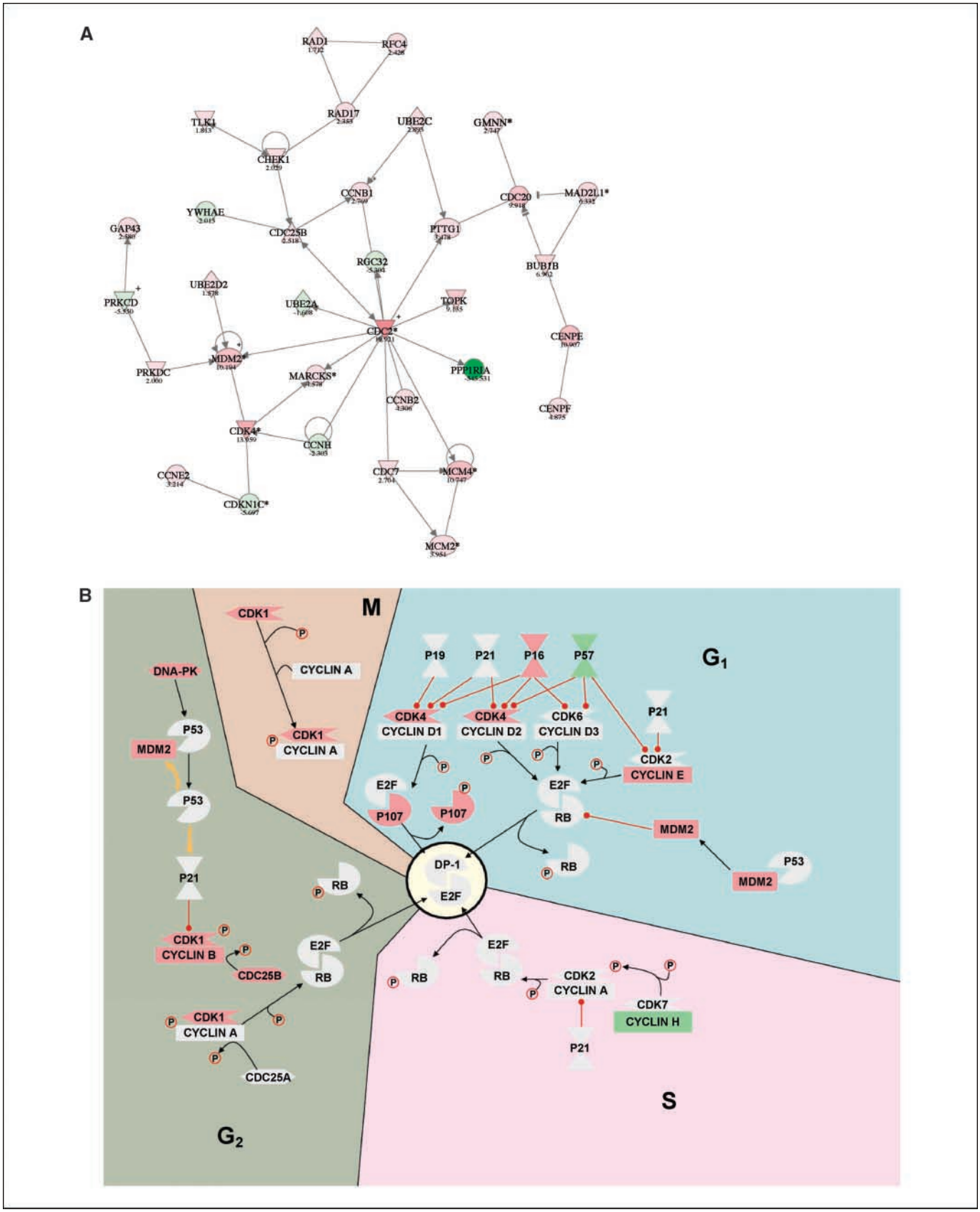

Figure 3. *A,* cell cycle and mitotic checkpoint gene interaction network in well-differentiated/dedifferentiated liposarcoma compared with normal fat. *Red,* overexpressed genes; *green,* underexpressed genes: the degree of color is proportional to the amount of differential expression. *B,* cell cycle regulation in well-differentiated/dedifferentiated liposarcoma.

nutlin whereas the NADIP cells remained resistant to the drug. The mechanism of decreased cell growth seems to be in part mediated by an induction of apoptosis as indicated by Annexin V labeling (Fig. 4*B*) and a G_2 cell cycle arrest (Fig. 4*C*). Although both cell lines are sensitive to the drug, this effect was greatest for the LS141 cell line with 48 h of drug exposure and only 5 μmol/L of nutlin. This increase in apoptosis in the LS141 cells can explain its increased sensitivity to single-agent drug therapy even among dedifferentiated liposarcoma cell lines.

We next elected to examine changes in MDM2, p53, and p21 expression in the three cell lines. For these studies the cell lines were treated with 2.5 to 10 μmol/L of nutlin for 24 h and then examined for changes in these molecular events. As shown in Fig. 5, nutlin induces p53 in both the LS141 and the DDLS cell lines. The interruption of the MDM2-p53 interaction also results in a significant increase in MDM2 by an established autoregulatory feedback loop (13, 14). This effect was greatest for the LS141 cell line and may be explained by the presence of a common polymorphism in codon 72 of p53 for LS141, which was not found in DDLS. This polymorphism has been associated with more efficient transcription of p53 and p21 (15) and may explain the increased sensitivity of LS141 cells to nutlin compared with the DDLS cell line. The increase in p53 induces p21 in the liposarcoma cell lines at nutlin concentrations as low as 2.5 μmol/L. In LS141 and DDLS cell lines, a nutlin concentration of 5 μmol/L activates the p53-p21 axis, resulting in a G_2 cell cycle arrest (Fig. 4*C*). In contrast, in the NADIP cells, in which MDM2 is not amplified and p53 is functional, 5 μmol/L nutlin do not result in increased expression of MDM2, p53, or p21 and there is no change in cell cycle or apoptosis. In the NADIP cells, increased expression of p53 is only seen at high nutlin concentrations (10 μmol/L) with minimal induction of p21. In summary, nutlin-3a, a small molecular antagonist of MDM2, preferentially activates the p53 pathway in dedifferentiated liposarcoma cell lines compared with NADIP cells, leading to a G_2 cell cycle arrest and apoptosis in liposarcoma cells. These results suggest that liposarcoma cells with MDM2 overexpression retain critical functionality in downstream p53-dependent apoptotic signaling pathways and that the growth suppressive effects of the p53 pathway is well preserved in liposarcoma and, in fact, substantially more pronounced than NADIPs in response to MDM2 antagonists.

Discussion

Mortality rates for patients with liposarcoma are highly heterogeneous and are largely dependent on the histologic subtype, location, tumor burden, and patient age (6, 7). Histologic subtype based on the morphologic appearance of the tumor is the most important prognostic factor for survival, yet prior studies have shown a high level of disagreement (25–40%) even among expert pathologists for histologic type (16, 17) and emphasize the need to develop new objective methods of liposarcoma classification. High-throughput transcriptional profiling using DNA microarrays provides tools to tackle this heterogeneity. Genome-wide expression studies of various cancers have identified subtypes of tumors previously unrecognized but biologically and clinically relevant with respect to morphologic features and prognosis (9, 10, 18–20). This is important because molecular distinct tumor subtypes represent different diseases that ideally would require different treatments. Most recently, particular subtypes of liposarcoma have been found to be associated with specific chromosomal translocations and specific cytogenetic abnormalities (21–23) and have been used to improve the accuracy of subtype classification when combined with morphology. However, cytogenetic analysis is labor intensive and remains difficult to uniformly apply to all samples because some subtypes do not grow well in short-term culture. Immunohistochemical analysis of MDM2 and CDK4 protein expression may help to discriminate benign lipomas characterized by 12q13-15 rearrangements from well-differentiated liposarcoma/atypical lipomatous tumors characterized by 12q13-15 amplification with overrepresentation of the CDK4 and MDM2 genes (24, 25). A recent study has shown that MDM2 and CDK4 immunoexpressions correlate closely with the gene amplification status in soft tissue tumors and show the utility of MDM2 and CDK4 immunostaining as helpful adjuncts to distinguish well-differentiated liposarcoma from benign adipose tumors and dedifferentiated liposarcoma from poorly differentiated sarcomas (26). However, amplification and overexpression of *CDK4, MDM2, GLI,* and *SAS* genes of the 12q13-15 region has been detected in 45% of leiomyosarcoma and 54% of rhabdomyosarcoma (27, 28) and has also been detected frequently in human parosteal osteosarcomas (29) and in 10% of Ewing's sarcoma (30). This suggests that the molecular deregulation of CDK4 and MDM2 is not specific for the well-differentiated/dedifferentiated liposarcoma subtypes.

To further improve subtype classification, we sought to develop a classifier based on gene expression monitoring to automatically discover the distinction between liposarcoma subtypes and normal fat samples. In this analysis we examine all three biological groups of liposarcoma, as well as lipoma and normal fat. Using an unsupervised hierarchical clustering of gene expression profiles, three main clusters are found that show significant differences with respect to both tumor differentiation and subtype. These results suggest that lipomatous tissues with similar histologic features of differentiation show similarities in gene expression. A 142-gene multiclass SVM-based classifier using 15 genes per pair-wise classifier was able to determine subtype with over 90% accuracy, and on an independent test set subtype was 86% of samples correctly. The high performance of this SVM-based classifier shows the promise of using a relatively small subset of genes to enhance the diagnostic accuracy of liposarcoma subtype based entirely on morphologic features.

Activation of cell cycle and checkpoint pathways in well-differentiated and dedifferentiated liposarcoma. The cyclin-CDK complexes serve as important regulators of key cell cycle transitions. The *cyclin D–CDK4/6* for G_1 progression (31), *cyclin E–CDK2* for G_1-S transition, *cyclin A–CDK2* for S-phase progression (32), and cyclin *A/B–CDC2* (*CDK1*) for entry into M phase (33). Figure 3*B* shows the interplay of key genes for regulating the stages of the cell cycle and how the measured alterations in key gene expression levels in the various phases of the cell cycle pathway can lead to uncontrolled growth and contribute to liposarcoma formation. The increased expression of the G_1-S phase regulators *CDK4* and *cyclin E* would serve to enhance the G_1-S transition. The universal CDI inhibitor *Kip2* (*p57, CDKN1C*), which inhibits all of the G_1 kinases (*CDK2, CDK4,* and *CDK6*), is 5-fold reduced in dedifferentiated liposarcoma compared with normal fat. The decrease in *p57* levels with progression from well-differentiated to dedifferentiated liposarcoma may account for the increase in cellular proliferation usually associated with dedifferentiated liposarcoma and may further enhance G_1-S transition in this subtype (34).

An important regulator of the G_2-M checkpoint, *CDC2,* is significantly overexpressed in all liposarcoma subtypes compared with normal fat based on microarray analysis (Table 1*A* and *B*;

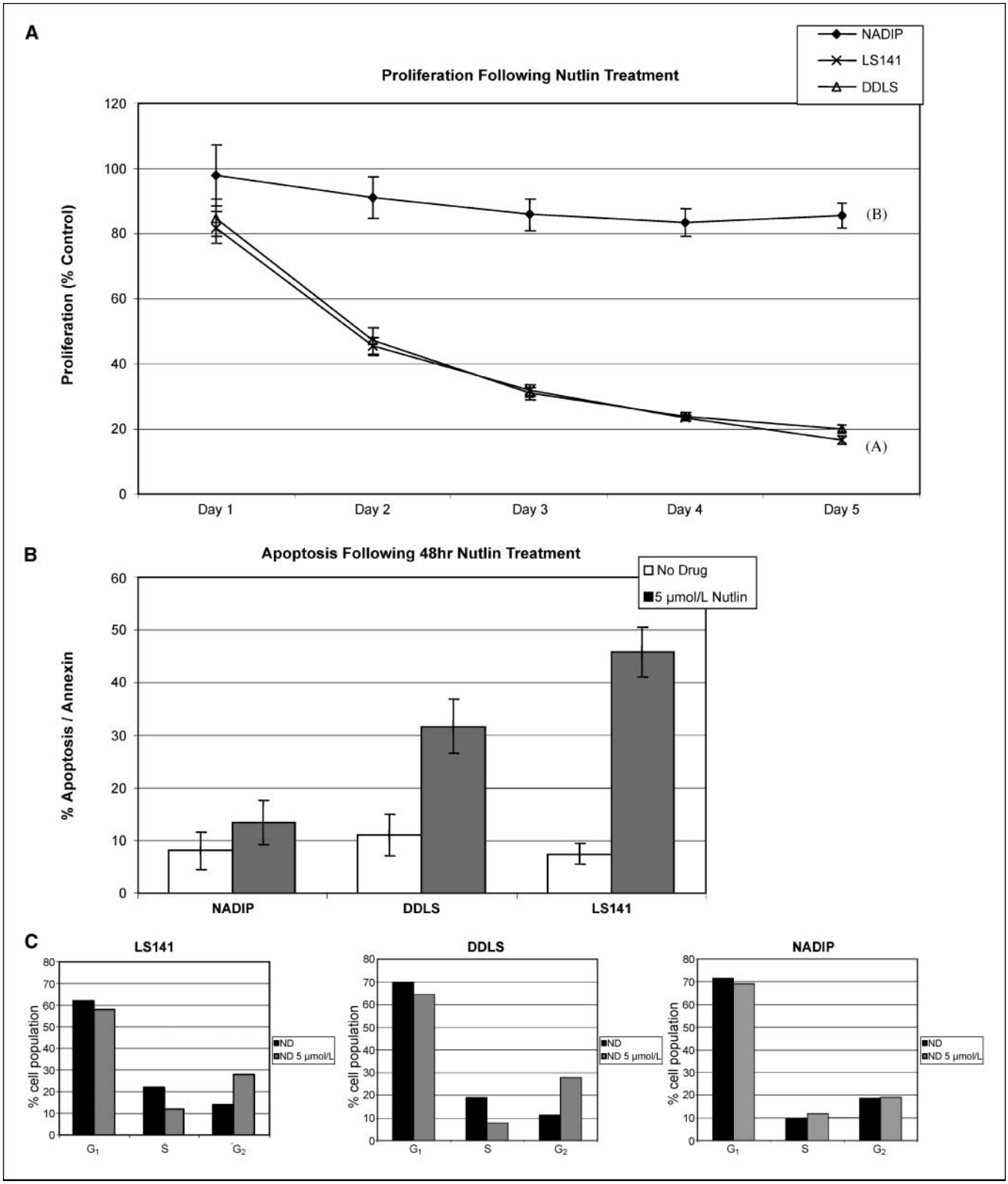

Figure 4. *A,* proliferation assay of the two dedifferentiated liposarcoma cell lines (*A*) with amplified MDM2 (LS141 and DDLS) and the NADIP cell line (*B*), which does not have amplified MDM2, which were treated with 5 μmol/L of nutlin-3 for 1 to 5 d, and cell viability was measured. LS141 and DDLS (*A*) showed 80% inhibition of proliferation after 5 d of treatment with nutlin-3 compared with NADIP cells (*B*), which were found to have only 15% inhibition of proliferation. *B,* exposure of LS141 and DDLS cells to 5 μmol/L nutlin-3 for 48 h resulted in a 3-fold and 5-fold increase in apoptosis over baseline levels, respectively, as indicated by Annexin V labeling. Although both cell lines are sensitive to the drug, this effect was greatest for the LS141 cell line. Exposure of NADIP cells to 5 μmol/L nutlin-3 for 48 h resulted in no change in apoptosis. *C,* effect of 5 μmol/L nutlin-3 on cell cycle distribution in LS141, DDLS, and NADIP cells. A G_2 cell cycle arrest was found in LS141 and DDLS cells after treatment with nutlin-3. In contrast, no change in cell cycle was seen in NADIP cells after nutlin-3 treatment.

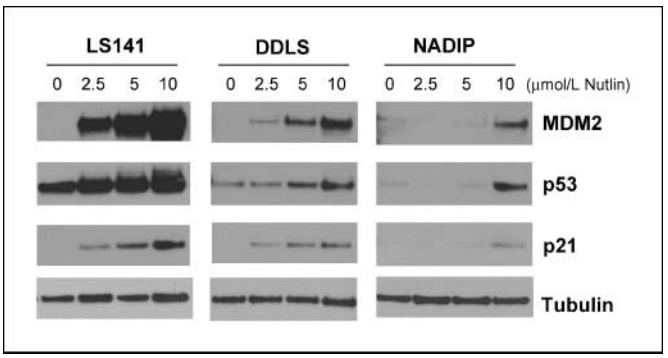

Figure 5. Western blot for MDM2, p53, and p21 after treatment with 2.5 to 10 μmol/L of nutlin for 24 h in dedifferentiated liposarcoma cell lines with amplified MDM2 and in a NADIP cell line with normal MDM2 expression.

Supplementary Tables S2–S4) and RT-PCR (Supplementary Fig. S2). As well-differentiated liposarcoma progresses to dedifferentiated liposarcoma, in addition to the substantial ~4-fold further increase in *CDC2* expression, there is a 3-fold increase in *cyclin B1* and 4-fold increase in *cyclin B2* expression compared with normal fat. However, additional factors besides *cyclin B* transcription rate are involved in regulating mitosis from G_2. In early G_2, inhibitory phosphorylation of CDC2 by wee1 is counteracted by the CDC25 phosphatase (35). *CDC25B* is 3-fold overexpressed in dedifferentiated liposarcoma compared with normal fat. CDC25 is phosphorylated and activated by cyclin B/CDC2 complexes. Studies using recombinant proteins suggest that a positive feed-back loop between CDC2 and CDC25 is necessary for the full activation of cyclin B/CDC2 that induces abrupt entry into mitosis *in vivo* (36).

Several of these differentially expressed cell cycle control genes serve as potential therapeutic targets in liposarcoma which are subtype specific. Based on the high-expression levels of *CDK4, cyclin E2, cyclin B1, cyclin B2,* and *CDC2* in well-differentiated and dedifferentiated liposarcoma compared with normal fat, one would predict that flavopiridol, a pan cyclin–dependent kinase inhibitor, which has been shown to bind to and directly inhibit cyclin B1–CDC2 kinase, CDK2, CDK4, and CDK6 should show increased antitumor activity in these liposarcoma subtypes. We are now evaluating in preclinical studies the activity of flavopiridol compounds in well-differentiated and dedifferentiated liposarcoma cell lines.

The mitotic checkpoint protein *MAD2* was found to be 6-fold, 10-fold, and 13-fold overexpressed in dedifferentiated, round cell, and pleomorphic liposarcoma, respectively, compared with normal fat (validated by real-time RT-PCR; see Supplementary Fig. S2). The low-grade liposarcoma subtypes, well differentiated and myxoid, were found to not overexpress *MAD2. MAD2* is a direct target of *E2F* and is aberrantly expressed in cells with defects in the Rb pathway (37, 38). Aberrant *MAD2* expression has been associated with checkpoint defects leading to aneuploidy. The spindle checkpoint serves to maintain genomic stability by preventing the onset of anaphase until all chromosomes are properly attached to the mitotic spindle. The MAD2 checkpoint protein is a key component of this checkpoint system because it inhibits the anaphase-promoting complex and its coactivator CDC20. Spindle damaging agents, such as paclitaxel (Taxol), stabilize microtubules, inducing a mitotic arrest and activating the spindle cell checkpoint before the subsequent sub-G_1 apoptosis (39). Recent work suggests that overexpression of MAD2 protein in checkpoint-defective cells enhances paclitaxel sensitivity (40, 41). We plan further studies to test the spindle checkpoint response in dedifferentiated liposarcoma cell lines so as to develop a strategy for fostering enhanced apoptosis after treatment with microtubule inhibitors, such as paclitaxel. Previous work has shown that flavopiridol enhances paclitaxel-induced apoptosis only when given after paclitaxel treatment (42). The elevated levels of *MAD2* in dedifferentiated, round cell, and pleomorphic liposarcoma may make these subtypes sensitive to paclitaxel therapy, either alone or in combination with flavopiridol.

MDM2 as a therapeutic target in liposarcoma subtypes that overexpress *MDM2*. In this study, we have shown that *MDM2* is overexpressed in well-differentiated and dedifferentiated liposarcoma compared with normal fat tissue and in dedifferentiated liposarcoma cell lines compared with normal human preadipocyte cells. Overproduction of MDM2 not only down-modulates p53 stability and function, inhibiting wild-type p53–mediated apoptosis, but also interacts physically and functionally with pRb and inhibits pRb growth regulatory function (43), leading to loss of the two main inhibitory systems of cell proliferation that act at the G_1-S and G_2-M checkpoints (see Fig. 3*B*). MDM2 facilitates the shift into S phase by activating E2F-1 (44). Activation of E2F-1 triggers dissociation of E2F-1–pRb complexes, which removes the block from G_1-S phase. Thus, amplification of *MDM2* in well-differentiated and dedifferentiated liposarcoma can function both to induce cell proliferation and enhance cell survival. Because *p53* mutations are relatively infrequent in liposarcoma subtypes with amplified *MDM2* (45, 46), we postulated that selective activation of p53 might offer an alternative therapeutic strategy for these liposarcoma subtypes, which are largely resistant to conventional chemotherapy. However, it is not known if p53-dependent apoptotic signaling is functionally intact in dedifferentiated liposarcoma cells and if this effect could be used to preferentially induce cell death in liposarcoma cells compared with NADIP cells. In this study, we report on the first molecular and functional analysis of the p53 pathway in dedifferentiated liposarcoma and NADIP cell lines using the recently developed MDM2 antagonist, nutlin-3a, as a specific p53 inducer (13).

Treatment of dedifferentiated liposarcoma cells with nutlin-3a at concentrations as low as 2.5 μmol/L results in increased levels of p53 protein and its downstream transcriptional targets *MDM2* and *p21.* Nutlin-3a treatment of two dedifferentiated liposarcoma cell lines resulted in significant induction of apoptosis and inhibition of proliferation associated with a G_2 cell cycle arrest. In contrast, NADIP cells following treatment with 2.5 to 5 μmol/L concentrations of nutlin-3a showed no apoptosis, cell cycle, or proliferative changes. For the normal adipocyte cells, induction of p53, p21, and MDM2 was seen only following treatment with high (10 μmol/L) concentrations of nutlin-3a. Thus, downstream p53 pathway signaling in dedifferentiated liposarcoma cell lines with overexpressed MDM2 seems to be much more pronounced than normal adipocyte cells and suggests that MDM2 antagonists, such as nutlin-3a, might serve as an effective therapeutics for liposarcomas with *MDM2* amplification and at the same time induce few antiproliferative or apoptotic effects on normal cells.

In summary, we have shown the utility of gene expression analysis for the diagnosis of liposarcoma subtype and how differential gene expression between liposarcoma tissue types and normal fat can be combined with bioinformatic pathway analysis to prioritize genes as potential therapeutic targets. Activation of cell cycle and checkpoint pathways in well-differentiated and dedifferentiated liposarcoma combined with MDM2 overexpression in these subtypes identified MDM2 as a

promising drug target. A highly specific MDM2 antagonist, nutlin-3a, results in substantial apoptosis in dedifferentiated liposarcoma cell lines that were not found in NADIP cells. These results further support the clinical development of MDM2 antagonists for the treatment of liposarcoma that overexpress MDM2 and show the promise of this transcriptional dataset to provide additional novel targets for drug discovery.

Acknowledgments

Received 2/12/2007; revised 4/11/2007; accepted 5/14/2007.

Grant support: Soft Tissue Sarcoma Program Project PO1 CA047179, Kristin Ann Carr Fund, and NIH T32 training grant CA09501 (E.B. Sambol).

The costs of publication of this article were defrayed in part by the payment of page charges. This article must therefore be hereby marked *advertisement* in accordance with 18 U.S.C. Section 1734 solely to indicate this fact.

The authors thank Lyubomir Vassilev (Discovery Oncology, Hoffmann-La Roche Inc.) for his helpful comments and suggestions.

References

1. Mack T. Sarcomas and other malignancies of soft tissue, retroperitoneum, peritoneum, pleura, heart, mediastinum and spleen. Cancer 1995;75:211–44.
2. Antonescu CR, Tschernyavsky SJ, Decuseara R, et al. Prognostic impact of P53 status, TLS-CHOP fusion transcript structure, and histological grade in myxoid liposarcoma: a molecular and clinicopathologic study of 82 cases. Clin Cancer Res 2001;7:3977–87.
3. Eilber FC, Eilber FR, Eckardt J, et al. The impact of chemotherapy on the survival of patients with high-grade primary extremity liposarcoma. Ann Surg 2004; 240:686–95; discussion 95–7.
4. Gebhard S, Coindre JM, Michels JJ, et al. Pleomorphic liposarcoma: clinicopathologic, immunohistochemical, and follow-up analysis of 63 cases: a study from the French Federation of Cancer Centers Sarcoma Group. Am J Surg Pathol 2002;26:601–16.
5. Kooby DA, Antonescu CR, Brennan MF, Singer S. Atypical lipomatous tumor/well-differentiated liposarcoma of the extremity and trunk wall: importance of histological subtype with treatment recommendations. Ann Surg Oncol 2004;11:78–84.
6. Singer S, Antonescu CR, Riedel E, Brennan MF. Histologic subtype and margin of resection predict pattern of recurrence and survival for retroperitoneal liposarcoma. Ann Surg 2003;238:358–70; discussion 70–1.
7. Dalal KM, Kattan MW, Antonescu CR, Brennan MF, Singer S. Subtype specific prognostic nomogram for patients with primary liposarcoma of the retroperitoneum, extremity, or trunk. Ann Surg 2006;244:381–91.
8. Eilber F, Eilber F, Eckardt J, et al. Ifosfamide based chemotherapy is associated with improved survival in patients with primary extremity synovial sarcoma. New Orleans (LA): ASCO; 2004.
9. Nielsen TO, West RB, Linn SC, et al. Molecular characterisation of soft tissue tumours: a gene expression study. Lancet 2002;359:1301–7.
10. Segal NH, Pavlidis P, Antonescu CR, et al. Classification and subtype prediction of adult soft tissue sarcoma by functional genomics. Am J Pathol 2003;163:691–700.
11. Fritz B, Schubert F, Wrobel G, et al. Microarray-based copy number and expression profiling in dedifferentiated and pleomorphic liposarcoma. Cancer Res 2002;62: 2993–8.
12. Shimoji T, Kanda H, Kitagawa T, et al. Clinicomolecular study of dedifferentiation in well-differentiated liposarcoma. Biochem Biophys Res Commun 2004; 314:1133–40.
13. Vassilev LT, Vu BT, Graves B, et al. *In vivo* activation of the p53 pathway by small-molecule antagonists of MDM2. Science 2004;303:844–8.
14. Tovar C, Rosinski J, Filipovic Z, et al. Small-molecule MDM2 antagonists reveal aberrant p53 signaling in cancer: implications for therapy. Proc Natl Acad Sci U S A 2006;103:1888–93.
15. Thomas M, Kalita A, Labrecque S, Pim D, Banks L, Matlashewski G. Two polymorphic variants of wild-type p53 differ biochemically and biologically. Mol Cell Biol 1999;19:1092–100.
16. Alvegard TA, Berg NO. Histopathology peer review of high-grade soft tissue sarcoma: the Scandinavian Sarcoma Group experience. J Clin Oncol 1989;7: 1845–51.
17. Coindre J, Trojani M, Contesso G, David M. Reproducibility of a histopathologic grading system for adult soft-tissue sarcoma. Cancer 1986;58:306–9.
18. Alizadeh AA, Eisen MB, Davis RE, et al. Distinct types of diffuse large B-cell lymphoma identified by gene expression profiling. Nature 2000;403:503–11.
19. Perou CM, Sorlie T, Eisen MB, et al. Molecular portraits of human breast tumours. Nature 2000;406: 747–52.
20. Schaner ME, Ross DT, Ciaravino G, et al. Gene expression patterns in ovarian carcinomas. Mol Biol Cell 2003;14:4376–86.
21. Bassett MD, Schuetze SM, Disteche C, et al. Deep-seated, well differentiated lipomatous tumors of the chest wall and extremities: the role of cytogenetics in classification and prognostication. Cancer 2005;103: 409–16.
22. Meis-Kindblom JM, Sjogren H, Kindblom LG, et al. Cytogenetic and molecular genetic analyses of liposarcoma and its soft tissue simulators: recognition of new variants and differential diagnosis. Virchows Arch 2001;439:141–51.
23. Sandberg AA. Updates on the cytogenetics and molecular genetics of bone and soft tissue tumors: liposarcoma. Cancer Genet Cytogenet 2004;155:1–24.
24. Dei Tos AP, Doglioni C, Piccinin S, et al. Coordinated expression and amplification of the MDM2, CDK4, and HMGI-C genes in atypical lipomatous tumours. J Pathol 2000;190:531–6.
25. Pilotti S, Della Torre G, Mezzelani A, et al. The expression of MDM2/CDK4 gene product in the differential diagnosis of well differentiated liposarcoma and large deep-seated lipoma. Br J Cancer 2000; 82:1271–5.
26. Binh MB, Sastre-Garau X, Guillou L, et al. MDM2 and CDK4 immunostainings are useful adjuncts in diagnosing well-differentiated and dedifferentiated liposarcoma subtypes: a comparative analysis of 559 soft tissue neoplasms with genetic data. Am J Surg Pathol 2005;29: 1340–7.
27. Ragazzini P, Gamberi G, Pazzaglia L, et al. Amplification of CDK4, MDM2, SAS and GLI genes in leiomyosarcoma, alveolar and embryonal rhabdomyosarcoma. Histol Histopathol 2004;19:401–11.
28. Anderson J, Gordon A, Pritchard-Jones K, Shipley J. Genes, chromosomes, and rhabdomyosarcoma. Genes Chromosomes Cancer 1999;26:275–85.
29. Wunder JS, Eppert K, Burrow SR, Gokgoz N, Bell RS, Andrulis IL. Co-amplification and overexpression of CDK4, SAS and MDM2 occurs frequently in human parosteal osteosarcomas. Oncogene 1999;18: 783–8.
30. Ladanyi M, Lewis R, Jhanwar SC, Gerald W, Huvos AG, Healey JH. MDM2 and CDK4 gene amplification in Ewing's sarcoma. J Pathol 1995;175:211–7.
31. Sherr CJ. G_1 phase progression: cycling on cue. Cell 1994;79:551–5.
32. Fang F, Newport JW. Evidence that the G_1-S and G_2-M transitions are controlled by different cdc2 proteins in higher eukaryotes. Cell 1991;66:731–42.
33. Riabowol K, Draetta G, Brizuela L, Vandre D, Beach D. The cdc2 kinase is a nuclear protein that is essential for mitosis in mammalian cells. Cell 1989;57: 393–401.
34. Gomez Lahoz E, Liegeois NJ, Zhang P, et al. Cyclin D- and E-dependent kinases and the p57(KIP2) inhibitor: cooperative interactions *in vivo*. Mol Cell Biol 1999;19: 353–63.
35. Russell P, Nurse P. cdc25+ functions as an inducer in the mitotic control of fission yeast. Cell 1986;45: 145–53.
36. Izumi T, Maller JL. Elimination of cdc2 phosphorylation sites in the cdc25 phosphatase blocks initiation of M-phase. Mol Biol Cell 1993;4:1337–50.
37. Nahle Z, Polakoff J, Davuluri RV, et al. Direct coupling of the cell cycle and cell death machinery by E2F. Nat Cell Biol 2002;4:859–64.
38. Ren B, Cam H, Takahashi Y, et al. E2F integrates cell cycle progression with DNA repair, replication, and G(2)/M checkpoints. Genes Dev 2002;16:245–56.
39. Jordan MA, Wendell K, Gardiner S, Derry WB, Copp H, Wilson L. Mitotic block induced in HeLa cells by low concentrations of paclitaxel (Taxol) results in abnormal mitotic exit and apoptotic cell death. Cancer Res 1996; 56:816–25.
40. Sudo T, Nitta M, Saya H, Ueno NT. Dependence of paclitaxel sensitivity on a functional spindle assembly checkpoint. Cancer Res 2004;64:2502–8.
41. Sihn CR, Suh EJ, Lee KH, Kim TY, Kim SH. p55CDC/hCDC20 mutant induces mitotic catastrophe by inhibiting the MAD2-dependent spindle checkpoint activity in tumor cells. Cancer Lett 2003;201: 203–10.
42. Motwani M, Delohery TM, Schwartz GK. Sequential dependent enhancement of caspase activation and apoptosis by flavopiridol on paclitaxel-treated human gastric and breast cancer cells. Clin Cancer Res 1999;5: 1876–83.
43. Xiao ZX, Chen J, Levine AJ, et al. Interaction between the retinoblastoma protein and the oncoprotein MDM2. Nature 1995;375:694–8.
44. Martin K, Trouche D, Hagemeier C, Sorensen TS, La Thangue NB, Kouzarides T. Stimulation of E2F1/DP1 transcriptional activity by MDM2 oncoprotein. Nature 1995;375:691–4.
45. Dei Tos AP, Doglioni C, Piccinin S, et al. Molecular abnormalities of the p53 pathway in dedifferentiated liposarcoma. J Pathol 1997;181:8–13.
46. Pilotti S, Della Torre G, Lavarino C, et al. Distinct mdm2/p53 expression patterns in liposarcoma subgroups: implications for different pathogenetic mechanisms. J Pathol 1997;181:14–24.

Gene Expression Profiling of Liposarcoma Identifies Distinct Biological Types/Subtypes and Potential Therapeutic Targets in Well-Differentiated and Dedifferentiated Liposarcoma

Samuel Singer, Nicholas D. Socci, Grazia Ambrosini, et al.

Cancer Res 2007;67:6626-6636.